International Journal of Control, Automation and Systems 19(8) (2021) 2784-2796
http://dx.doi.org/10.1007/s12555-020-0423-8
ISSN:1598-6446 eISSN:2005-4092
http://www.springer.com/12555

Adaptive Safety Motion Control for Underactuated Hovercraft Using Improved Integral Barrier Lyapunov Function

Mingyu Fu, Tan Zhang*, and Fuguang Ding

Abstract: In this paper, we investigate the problem of safety motion control for an underactuated hovercraft from subject to safety constraint on the states, and model uncertainties. First, a new improved integral barrier Lyapunov function is proposed to constrain the surge speed, it can guarantee the lower limit of the surge speed is above the resistance hump speed in order to prevent loss of course stability. Second, to ensure that the heading remains within the pre-specified safety boundary, a time-varying integral barrier Lyapunov function is introduced to avoid the violation of the constraint. Third, we constrain the yaw angular velocity to the interior of the time-varying safety boundary is related to the surge speed to aim at performing the safety turning under the high speed. To deal with model uncertainties, an adaptive parameter approximation algorithm is designed to estimate it. With the help of Lyapunov's stability theory, it can be proved that all the tracking errors are uniformly ultimately bounded. Finally, results from some simulation studies verify the effectiveness and universality of the proposed scheme.

Keywords: Improved integral barrier function, safety motion control, time-varying constraints, underactuated hovercraft.

1. INTRODUCTION

The hovercraft is viewed as a high-performance amphibious marine craft because its hull can be totally lifted up by a pressurized air cushion which is produced by a flexible skirt system [1]. Accordingly, the hovercraft has a higher speed than a normal surface vessel. In recent decades, due to its superior high speed and unique amphibious performance, the hovercraft has more and more attention in both military and civil fields.

What is particularly noteworthy is that the hovercraft has very little contact with the sailing surface. It is easy to generate a large roll angle and drift angle so that the hovercraft runs in a dangerous situation. Moreover, the lateral component of the air cushion force under large roll angle results in the hovercraft drifting sideways and losing course stability [2]. The roll motion occurs always when the hovercraft is turning and is more violent with the increase of the turn rate. Therefore, the turn rate must be constrained within the safety boundary. From a detailed review of the available literature about the motion control of the hovercraft [1–6], the surge speed has never been constrained. However, the surge speed is influenced by the resistance hump of the hovercraft. The course stability will become poor when the surge speed is lower than the resistance hump speed. Hence, the surge speed needs to be constrained above the resistance hump speed for holding better stability. Thus, it is necessary to constrain states of the hovercraft for ensuring safe navigation.

In the past decades, in order to deal with the problem of the state constraints in control systems, numerous significant methods have been proposed through the efforts of the researchers such as moving-horizon optimal control [7,8], artificial potential fields [9,10], model-predictive control [11,12], etc. In the moving-horizon optimal control schemes, the control input is obtained by solving an open-loop finite-horizon optimal control problem online, which can be applied effectively to linear systems [8]. The artificial potential field method can construct dynamic constrained motion with observed state information by defining appropriate repulsive and attractive artificial potential fields. In [11], the model-predictive control method is proposed to address the path following of marine surface vessels with input and state constraints. The problem of guaranteeing Quality of Service using optimal buffer allocation is addressed in [13]. Furthermore, the model predictive control approach is proposed to compute the optimal buffer with respect to a real-world dataset accounting for the expected data traffic volume for a predefined set of business users belonging to a mobile network scenario. The approach of a quaternion orientation based quadrotor that can be controlled by model predictive con-

Manuscript received June 10, 2020; revised October 26, 2020; accepted December 3, 2020. Recommended by Editor Kyoung Kwan Ahn. This work is supported by the National Natural Science Foundation of China under grant 51309062.

Mingyu Fu, Tan Zhang, and Fuguang Ding are with the College of Automation, Harbin Engineering University, Heilongjiang Province 150001, China (e-mails: {fumingyu, zhangtantan, dingfuguang}@hrbeu.edu.cn).
* Corresponding author.

trol is proposed in [14]. In [14], the main contribution is to present a novel cost function for model predictive control because, by definition, quaternion error is remarkably different from the Euler angle's attitude error. A robust model predictive control approach-based trajectory tracking control for an underactuated two-wheeled inverted pendulum vehicle with various physical constraints is proposed in [15]. In [16], a Lyapunov-based predictive tracking controller for nonholonomic wheeled robots with control input constraints is proposed to address the global position and orientation tracking problem of the robot. However, solving complex nonlinear optimizations brings difficulties for applying the above methods to real-time control.

Recently, considering the fact that practical systems are subjected to constraints in the form of safety requirement, output, and state, the barrier Lyapunov function-based control schemes are proposed [17–21]. In [22], *log*-type barrier Lyapunov function is introduced to guarantee the full-states stay within pre-specified time-invariant constraint boundaries. A *log*-type barrier Lyapunov function is used in [23] to tackle the trajectory tracking control problem for an underactuated autonomous underwater vehicle with time-invariant constraints on system output. A *tan*-type barrier Lyapunov function-based controller is developed to handle time-varying constraints on the tracking errors [24,25]. However, the above *log*-type and *tan*-type barrier Lyapunov function cannot constrain directly the system states, accordingly, which need an additional mapping to state space. An integral barrier Lyapunov function (iBLF) allowing the system state constraints to be mixed with the error terms is proposed in [26,27] to directly constrain the state signals. However, the above iBLFs only can constrain the states to the interior of a region containing zero, and therefore cannot meet the constraint on the surge speed in this paper.

Motivated by the above-mentioned observations, an improved iBLF-based adaptive safety motion control for an underactuated hovercraft is proposed that ensures safe navigation and deals with the model uncertainties. In particular, the constraint on the surge speed using improved iBLF in this paper has been unprecedented. Accordingly, the contributions of this study are summarized as follows:

1) Unlike the existing iBLF-based constraint scheme in [26–31], the proposed improved iBLF-based motion control scheme can guarantee the surge speed exceeds always the resistance hump speed, namely the hovercraft sails at high speed to ensure course stability.

2) Based on time-varying iBLF, we constrain the yaw angular velocity to the interior of a time-varying safety boundary is related to the surge speed to aim at performing the safety turning under the high speed.

3) To address the model uncertainties, an adaptive parameter estimation algorithm is incorporated with the control scheme. It is proven that the proposed control schemes are universal and easy to implement. The simulation results show the superiority and universality of the proposed strategies across various scenarios.

The remainder of this paper is arranged as follows: The preliminaries and problem formulation are given in Section 2. Section 3 is devoted to developing the adaptive safety motion controllers for a hovercraft. Numerical simulation results are shown in Section 4. Section 5 concludes the work of this paper.

2. PRELIMINARIES AND PROBLEM FORMULATION

2.1. Model description of a hovercraft

Neglecting the pitch and heave motion, four degrees of freedom model of the hovercraft shown in Fig. 1 with model uncertainties can be described as follows:

$$\begin{cases} \dot{x} = u\cos\psi - v\sin\psi\cos\phi, \\ \dot{y} = u\sin\psi + v\cos\psi\cos\phi, \\ \dot{\phi} = p, \\ \dot{\psi} = r\cos\phi, \\ \dot{u} = vr + F_{xD0}/m_0 + \Theta_u^T f_u(\dot{\eta},\eta) + \tau_u/m_0, \\ \dot{v} = -ur + F_{yD0}/m_0 + \Theta_v^T f_v(\dot{\eta},\eta), \\ \dot{p} = M_{xD0}/J_{x0} + \Theta_p^T f_p(\dot{\eta},\eta), \\ \dot{r} = M_{zD0}/J_{z0} + \Theta_r^T f_r(\dot{\eta},\eta) + \tau_r/J_{z0}, \end{cases} \tag{1}$$

where x, y, ϕ, ψ signify positions and attitudes of the hovercraft in the earth-fixed frame, u, v, p, r denote speeds and angular velocities. m_0, J_{x0}, J_{z0} are mass and moment of inertia, τ_u, τ_r represent control inputs. F_{xD0}, F_{yD0}, M_{xD0}, M_{zD0} are the total drags of the known model. Please refer to [2,32] for details of the drags. $\Theta_u \in R^{n_u}$, $\Theta_v \in R^{n_v}$, $\Theta_p \in R^{n_p}$, $\Theta_r \in R^{n_r}$ denote unknown constant vectors with known dimensions n_u, n_v, n_p, n_r. The model uncertainties $F_u = \theta_u^T f_u(\dot{\eta},\eta)$, $F_v = \theta_v^T f_v(\dot{\eta},\eta)$, $F_p = \theta_p^T f_p(\dot{\eta},\eta)$ and $F_r = \theta_r^T f_r(\dot{\eta},\eta)$ with $f_u = [vr, u]^T \in R^{n_u}$, $f_v = [ur, v]^T \in R^{n_v}$, $f_p = [vr, p]^T \in R^{n_p}$ and $f_r = [vu, r]^T \in R^{n_r}$ representing the known smooth vector functions, and $\eta = (u, v, p, r)$ denoting the independent variable of nonlinear functions f_u, f_v, f_p, and f_r. The model uncertainties are selected as $F_u = 0.2vr + 0.1u$ and $F_r = 0.1uv + 0.3r$. And the

Fig. 1. Three dimensional model of the hovercraft. Picture is from the international cooperation project of authors.

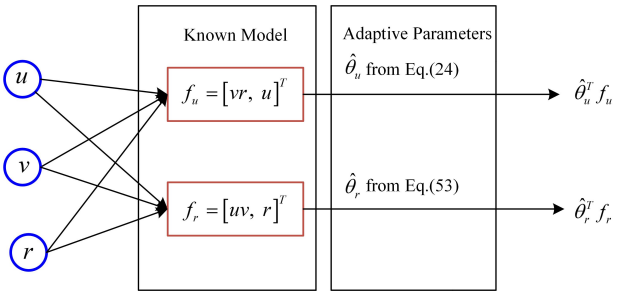

Fig. 2. Structure of the adaptive parameter estimation.

structure of the adaptive parameter estimation is shown in Fig. 2. The adaptive updating laws will be given later.

2.2. Preliminaries

In order to guarantee the time-varying safety constraints on the heading angle and yaw angular velocity of the hovercraft, the time-varying iBLF [27] is introduced as

$$V_i(e_i,k_{iH},i_d)=\int_0^{e_i}\frac{\sigma k_{iH}^2}{k_{iH}^2-(\sigma+i_d)^2}d\sigma, \tag{2}$$

where $e_i=i-i_d$ with i_d being a continuously differentiable desired target satisfying $|i_d|<k_{iH}$, $i=\psi,r$. It is clear that V_i is a continuously positive differentiable functional over the set $\Omega_i=\{i:|i|<k_{iH}\}$.

Assumption 1: The desired target values are set to satisfy $|i_d|<k_{iH}$, $i=\psi,r$.

Theorem 1: $V_i(e_i,k_{iH},i_d)$ is a continuously positive differentiable functional over the set Ω_i and satisfies always the following inequality:

$$\frac{e_i^2}{2}\le V_i\le\frac{k_{iH}^2e_i^2}{k_{iH}^2-i^2}. \tag{3}$$

Proof: Please refer to Appendix A in [27]. □

Remark 1: In the previous works applying iBLF [27–31], the constraint on the system states is time-invariant. However, for many practical systems [33], the constraint on the system states is time-varying. In (2), k_{iH} is a time-varying function and signifies safety limit of the system states. Therefore, it is practically significant to extend the previous iBLF-based controller designs for the system with time-varying state constraints.

To guarantee that the hovercraft sails at a safe speed, namely, the surge speed must be greater than the resistance hump speed, a new improved iBLF is proposed for the first time in this paper as

$$V_u(e_u,k_{uL},u_d)=\int_0^{e_u}\frac{\sigma(\sigma+u_d)^2}{(\sigma+u_d)^2-k_{uL}^2}d\sigma, \tag{4}$$

where $e_u=u-u_d$ and u_d is a continuously positive differentiable function or constant. It is obvious that V is a continuously positive differentiable functional over the set $\Omega_u:=\{u:u>k_{uL}\}$.

Assumption 2: The desired target value is set to satisfy $u_d>k_{uL}$.

Theorem 2: The functional $V_u(e_u,k_{uL},u_d)$ over the set Ω_u, designed in this paper, satisfies

$$\frac{e_u^2}{2}\le V_u(e_u,k_{uL},u_d)\le\frac{u^2e_u^2}{u^2-k_{uL}^2}. \tag{5}$$

Proof: The proof process is divided into two steps. First step, we prove that $V_{u0}(e_u,k_{uL},u_d)\le\frac{u^2e_u^2}{u^2-k_{uL}^2}$ holds. Define function $p(\sigma)=\sigma(\sigma+u_d)^2\Big/\Big((\sigma+u_d)^2-k_{uL}^2\Big)$, then the partial derivative $\partial p/\partial\sigma$ over the set Ω_u is

$$\frac{\partial p}{\partial\sigma}=\frac{\Big((\sigma+u_d)^3-k_{uL}^2(\sigma+u_d)-2k_{uL}^2\sigma\Big)(\sigma+u_d)}{\Big((\sigma+u_d)^2-k_{uL}^2\Big)^2}. \tag{6}$$

Define $p_\sigma=\Big((\sigma+u_d)^3-k_{uL}^2(\sigma+u_d)-2k_{uL}^2\sigma\Big)(\sigma+u_d)$. When $\sigma<0$, we know that $-2k_{uL}^2\sigma>0$ and $(\sigma+u_d)^3-k_{uL}^2(\sigma+u_d)>0$ in the set $\sigma+u_d>k_{uL}$, accordingly, $\partial p/\partial\sigma>0$ holds. When $\sigma>0$, we have

$$\begin{aligned}p_\sigma&=\big((\sigma^2+2\sigma u_d+u_d^2-k_{uL}^2)(\sigma+u_d)-2k_{uL}^2\sigma\big)(\sigma+u_d)\\&=\big(\sigma^3+3\sigma^2u_d+2\sigma\left(u_d^2-k_{uL}^2\right)\big)(\sigma+u_d)\\&\quad+\left(u_d^2-k_{uL}^2\right)(\sigma+u_d)^2.\end{aligned} \tag{7}$$

This means that $\partial p/\partial\sigma$ is positive for $u_d>k_{uL}$ in the set $\sigma+u_d>k_{uL}$. According to that $p(\sigma)$ is monotonically increasing function of variable σ in the set $\sigma+u_d>k_{uL}$, and $p(0)=0$, the following inequality holds

$$\int_0^{e_u}p(\sigma)d\sigma\le e_up(e_u)=\frac{e_u^2u^2}{u^2-k_{uL}^2}. \tag{8}$$

Second step, we prove that $\frac{e_u^2}{2}\le V_u(e_u,k_{uL},u_d)$ holds. First off, define the function:

$$g(e_u)=\int_0^{e_u}\frac{\sigma(\sigma+u_d)^2}{(\sigma+u_d)^2-k_{uL}^2}d\sigma-\frac{e_u^2}{2}, \tag{9}$$

the partial derivative of (9) is $\partial g(e_u)/\partial e_u=e_uk_{uL}^2/(u^2-k_{uL}^2)$, we can easily obtain that $\partial g(e_u)/\partial e_u<0$ when $e_u<0$ and $\partial g(e_u)/\partial e_u>0$ when $e_u>0$ over the compact set Ω_u. Furthermore, we have $g(e_u)=0$ when $e_u=0$. Accordingly, $g(e_u)\ge0$ always holds over the set Ω_u, namely, $\int_0^{e_u}\frac{\sigma(\sigma+u_d)^2}{(\sigma+u_d)^2-k_{uL}^2}d\sigma\ge\frac{e_u^2}{2}$. The proof of Theorem 2 is completed. □

Assumption 3: The initial values of the system states satisfy $u(0)>k_{uL}$, $|\psi(0)|<k_{\psi H}$ and $|r(0)|<k_{rH}$.

Remark 2: The existing iBLF can only constrain system states within a range around zero. However, in order to meet the practical requirement that some system states need to be greater than the safety value, such as hovercraft's surge speed is required to exceed resistance hump speed, the new improved iBLF is proposed to solve this kind of problem in this paper.

Theorem 3: For any positive constant k_l, define $\chi := \{x \in R : x > k_l\} \subset R$ and $\mathrm{N} := R^l \times \chi \subset R^{l+1}$ as open sets. Consider the following system:

$$\dot{\eta} = h(\eta, t), \tag{10}$$

where $\eta := [\omega, x]^T \in \mathrm{N}$ with $\omega = \begin{bmatrix} \omega_1 \\ \cdots \\ \omega_l \end{bmatrix}^T \in R^l$ being the free states, and $h : R_+ \times \mathrm{N} \to R^{l+1}$ is piecewise continuous with respect to t, locally Lipschitz with respect to η and uniformly in t, on $R_+ \times \mathrm{N}$. Suppose that there are functions $U : R^l \to R_+$ and $V_x : \chi \to R_+$ are positive definite and continuously differentiable in their respective domains, such that

$$V_x(x) \to \infty \ \text{ as } \ x \to k_l, \tag{11}$$

$$\gamma_1(\|\omega\|) \le U(\omega) \le \gamma_2(\|\omega\|), \tag{12}$$

where γ_1 and γ_2 are class k_∞ functions. Assign $V(\eta) = V_x + U$ and the initial value satisfies $x(0) \in \chi$. If the derivative of V with respect to η satisfies

$$\dot{V} = \frac{\partial V}{\partial \eta} h \le -\mu V + \lambda, \ \ \eta \in \mathrm{N}, \tag{13}$$

where μ and λ are positive constants, then ω is bounded and $x(t) \in \chi$, $\forall t \in [0, \infty)$.

Proof: We can easily know that the maximal solution $\eta(t)$ as $t \in [0, \tau_{\max})$ is existent and unique according to conditions on h. Considering the initial condition $x(0) \in \chi$, we have that $V_x(x(0))$ and $V(\eta(0))$ exist. Integrating both sides of (13), we have $V(\eta(t)) \le V(\eta(0)) + \lambda/\mu, t \in [0, \tau_{\max})$. According to $V(\eta) = V_x + U$ with V_x being a positive function, we obtain that V_x is bounded as $t \in [0, \tau_{\max})$. As $V_x \to \infty$ only if $x \to k_l$. In view of the boundedness of V_x, we have $x > k_l$, $t \in [0, \tau_{\max})$. Therefore, there exists a compact subset $\mathrm{K} \subset \mathrm{N}$ such that the maximal solution of (10) satisfies $\eta(t) \in \mathrm{K}, t \in [0, \tau_{\max})$. However, the domain of definition of $\eta(t)$ is $t \in [0, \infty)$, so we can obtain that $x(t) \in \chi, t \in [0, \infty)$. This completes the proof. □

Remark 3: Theorem 3 proposed in this paper is similar to Lemma 3 in [27] is aimed at completing the stability analysis of the constrained system. However, there exist some differences between them. Lemma 3 in [27] is only applied to prove the system state x can be constrained within a range containing zero, like $|x| < k$, $k > 0$. But the proposed Theorem 3 devotes to analyze that the lowest safety boundary of the system state x is ensured, for example, $x > k$, $k > 0$.

3. MOTION CONTROL DESIGN

3.1. Surge speed control

We define the surge speed tracking error and calculate its derivative as follows:

$$\begin{aligned} e_u &= u - u_d, \\ \dot{e}_u &= vr + \frac{F_{xD0}}{m_0} + \Theta_u^T f_u(\dot{\eta}, \eta) + \frac{\tau_u}{m_0} - \dot{u}_d, \end{aligned} \tag{14}$$

where u_d is desired surge speed.

In order to guarantee the surge speed is above resistance hump speed in the moving process, namely, $u > k_{uL}$ with k_{uL} being a positive time-varying lower bound constraint on the surge speed, we design a greatest lower bound-guaranteed iBLF for the first time as follows:

$$V_{u0}(e_u, k_{uL}, u_d) = \int_0^{e_u} \frac{\sigma(\sigma + u_d)^2}{(\sigma + u_d)^2 - k_{uL}^2} d\sigma. \tag{15}$$

For the sake of convenience in writing, we define $V_{u0}(\cdot) \overset{def}{=} V_{u0}(e_u, k_{uL}, u_d)$.

The derivative of (15) with respect to time is

$$\begin{aligned} \dot{V}_{u0}(\cdot) =& \frac{\partial V_u}{\partial e_u}\dot{e}_u + \frac{\partial V_u}{\partial u_d}\dot{u}_d + \frac{\partial V_u}{\partial k_{uL}}\dot{k}_{uL} \\ =& \frac{e_u u^2}{u^2 - k_{uL}^2}\dot{e}_u + e_u\left(\frac{u^2}{u^2 - k_{uL}^2} + l_{u_d}\right)\dot{u}_d \\ &+ e_u(l_{\partial ku1} + l_{\partial ku2} - l_{\partial ku3})\dot{k}_{uL}, \end{aligned} \tag{16}$$

where

$$l_{u_d} = \frac{1}{2}\frac{k_{uL}}{e_u}\ln\left(\frac{(u + k_{uL})(u_d - k_{uL})}{(u - k_{uL})(u_d + k_{uL})}\right), \tag{17}$$

$$l_{\partial ku1} = \frac{k_{uL}}{e_u}\ln\left(\frac{u^2 - k_{uL}^2}{u_d^2 - k_{uL}^2}\right), \tag{18}$$

$$l_{\partial ku2} = \frac{u_d}{2e_u}\ln\left(\frac{(u + k_{uL})(u_d - k_{uL})}{(u - k_{uL})(u_d + k_{uL})}\right), \tag{19}$$

$$l_{\partial ku3} = \frac{k_{uL} u}{u^2 - k_{uL}^2}. \tag{20}$$

By substituting (14) into (16), we have

$$\begin{aligned} \dot{V}_{u0}(\cdot) =& \frac{e_u u^2}{u^2 - k_{uL}^2}\left(vr + \frac{F_{xD0}}{m_0} + \Theta_u^T f_u + \frac{\tau_u}{m_0} - \dot{u}_d\right) \\ &+ e_u\left(\frac{u^2}{u^2 - k_{uL}^2} + l_{u_d}\right)\dot{u}_d - e_u l_{\partial ku3}\dot{k}_{uL} \\ &+ e_u(l_{\partial ku1} + l_{\partial ku2})\dot{k}_{uL}. \end{aligned} \tag{21}$$

According to (21), the surge control law is designed as follows:

$$\tau_u^* = m_0\left(-k_u e_u - vr - \frac{F_{xD0}}{m_0} - \Theta_u^T f_u - \frac{u^2-k_{uL}^2}{u^2}l_{u_d}\dot{u}_d - \frac{u^2-k_{uL}^2}{u^2}\left(l_{\partial ku1}+l_{\partial ku2}-l_{\partial ku3}\right)\dot{k}_{uL}\right), \tag{22}$$

where k_u is a positive constant. However, there is an unknown term in control law (22), therefore τ_u^* can't be applied directly to the actual system. An adaptive algorithm is utilized to approximate the uncertainty. The adaptive surge control law is designed as

$$\tau_u = m_0\left(-k_u e_u - vr - \frac{F_{xD0}}{m_0} - \hat{\Theta}_u^T f_u - \frac{u^2-k_{uL}^2}{u^2}l_{u_d}\dot{u}_d - \frac{u^2-k_{uL}^2}{u^2}\left(l_{\partial ku1}+l_{\partial ku2}-l_{\partial ku3}\right)\dot{k}_{uL}\right), \tag{23}$$

where $\hat{\Theta}_u$ signifies the estimation value of Θ_u with $\tilde{\Theta}_u = \Theta_u - \hat{\Theta}_u$ being the estimation error. Then we design the adaptive updating law as

$$\dot{\hat{\Theta}}_u = \Gamma_u\left(\frac{e_u u^2}{u^2-k_{uL}^2}f_u - \sigma_u\hat{\Theta}_u\right), \tag{24}$$

where $\Gamma_u \in R^{n_u\times n_u}$ is a positive definite diagonal matrix and σ_u is a positive design constant.

Next, let's discuss whether the control law τ_u is well defined when $e_u = 0$ or $e_u \neq 0$.

Remark 4: According to $u_d > k_{uL}$ in Assumption 2 and considering (17), (18) and (19), l_{u_d}, $l_{\partial ku1}$ and $l_{\partial ku2}$ are well defined and bounded when $e_u \neq 0$. When $e_u = 0$, since

$$\lim_{e_u\to 0} l_{u_d} = -\frac{k_{uL}^2}{u_d^2-k_{uL}^2}, \tag{25}$$

$$\lim_{e_u\to 0} l_{\partial ku1} = \frac{2k_{uL}u_d}{u_d^2-k_{uL}^2}, \tag{26}$$

$$\lim_{e_u\to 0} l_{\partial ku2} = -\frac{k_{uL}u_d}{u_d^2-k_{uL}^2}, \tag{27}$$

we have that l_{u_d}, $l_{\partial ku1}$ and $l_{\partial ku2}$ are well defined and bounded as well. Therefore, we can obtain that the control law τ_u is well defined whether $e_u = 0$ or $e_u \neq 0$.

Next, we will use the control law τ_u to prove the stability of the motion system whether $e_u = 0$ or $e_u \neq 0$.

Select the following candidate Lyapunov function:

$$V_u = V_{u0}(\cdot) + \frac{1}{2}\tilde{\Theta}_u^T\Gamma_u^{-1}\tilde{\Theta}_u. \tag{28}$$

By using (23) and (24), we can get the time derivative of (28) as

$$\begin{aligned}\dot{V}_u =& -k_u\frac{u^2e_u^2}{u^2-k_{uL}^2} + \sigma_u\tilde{\theta}_u^T\hat{\theta}_u\\ =& -k_u\frac{u^2e_u^2}{u^2-k_{uL}^2} + \sigma_u\tilde{\theta}_u^T\theta_u - \sigma_u\tilde{\theta}_u^T\tilde{\theta}_u\\ \leq& -k_u\frac{u^2e_u^2}{u^2-k_{uL}^2} + \frac{\sigma_u}{2}\tilde{\theta}_u^T\tilde{\theta}_u + \frac{\sigma_u}{2}\theta_u^T\theta_u.\end{aligned} \tag{29}$$

The result in (29) will be applied to the stability analysis of the motion system in Subsection 3.4. Furthermore, the condition of $e_u = 0$ is not used to prove the stability of the system.

3.2. Heading control

Unlike the design of the surge speed control law in subsection 3.1, this subsection introduces time-varying iBLF to ensure that the hovercraft sails in prescribed safety heading angles, namely, $|\psi| < k_{\psi H}$ with $k_{\psi H}$ being a positive time-varying function.

We define heading tracking error and take its derivative:

$$\begin{aligned}e_\psi &= \psi - \psi_d,\\ \dot{e}_\psi &= \dot{\psi} - \dot{\psi}_d = r\cos\phi - \dot{\psi}_d.\end{aligned} \tag{30}$$

The time-varying iBLF is constructed as

$$V_\psi\left(e_\psi, k_{\psi H}, \psi_d\right) = \int_0^{e_\psi}\frac{\sigma k_{\psi H}^2}{k_{\psi H}^2-(\sigma+\psi_d)^2}d\sigma. \tag{31}$$

Define $V_\psi(\cdot) \overset{def}{=} V_\psi\left(e_\psi, k_{\psi H}, \psi_d\right)$.
The time derivative of $V_\psi(\cdot)$ is given by

$$\begin{aligned}\dot{V}_\psi(\cdot) =& \frac{k_{\psi H}^2 e_\psi}{k_{\psi H}^2-\psi^2}\dot{e}_\psi + e_\psi\left(\frac{k_{\psi H}^2}{k_{\psi H}^2-\psi^2} - l_{\psi_d}\right)\dot{\psi}_d\\ &+ e_\psi\left(l_{\partial k\psi 1} - l_{\partial k\psi 2} + l_{\partial k\psi 3}\right)\dot{k}_{\psi H}\\ =& \frac{k_{\psi H}^2 e_\psi}{k_{\psi H}^2-\psi^2}\left(r\cos\phi - \dot{\psi}_d\right)\\ &+ e_\psi\left(\frac{k_{\psi H}^2}{k_{\psi H}^2-\psi^2} - l_{\psi_d}\right)\dot{\psi}_d\\ &+ e_\psi\left(l_{\partial k\psi 1} - l_{\partial k\psi 2} - l_{\partial k\psi 3}\right)\dot{k}_{\psi H},\end{aligned} \tag{32}$$

where

$$l_{\psi_d} = \frac{k_{\psi H}}{2e_\psi}\ln\frac{\left(k_{\psi H}+\psi\right)\left(k_{\psi H}-\psi_d\right)}{\left(k_{\psi H}-\psi\right)\left(k_{\psi H}+\psi_d\right)}, \tag{33}$$

$$l_{\partial k\psi 1} = \frac{k_{\psi H}}{e_\psi}\ln\left(\frac{k_{\psi H}^2-\psi_d^2}{k_{\psi H}^2-\psi^2}\right), \tag{34}$$

$$l_{\partial k\psi 2} = \frac{1}{2}\frac{\psi_d}{e_\psi}\ln\frac{\left(k_{\psi H}+\psi\right)\left(k_{\psi H}-\psi_d\right)}{\left(k_{\psi H}-\psi\right)\left(k_{\psi H}+\psi_d\right)}, \tag{35}$$

$$l_{\partial k\psi 3} = \frac{k_{\psi H}\psi}{k_{\psi H}^2-\psi^2}. \tag{36}$$

Remark 5: In view of $|\psi_d| < k_{\psi H}$ in Assumption 1 and considering (33), (34) and (35), l_{ψ_d}, $l_{\partial k\psi 1}$ and $l_{\partial k\psi 2}$ are

well defined when $e_\psi \neq 0$. When $e_\psi = 0$, since

$$\lim_{e_\psi \to 0} l_{\psi_d} = \frac{k_{\psi H}^2}{k_{\psi H}^2 - \psi_d^2}, \tag{37}$$

$$\lim_{e_\psi \to 0} l_{\partial k\psi 1} = \frac{2k_{\psi H}\psi_d}{k_{\psi H}^2 - \psi_d^2}, \tag{38}$$

$$\lim_{e_\psi \to 0} l_{\partial k\psi 2} = \frac{k_{\psi H}\psi_d}{k_{\psi H}^2 - \psi_d^2}, \tag{39}$$

we have that l_{ψ_d}, $l_{\partial k\psi 1}$ and $l_{\partial k\psi 2}$ are well defined as well.

The virtual control law r_d as stability function is given by

$$r_d = \left(-k_\psi e_\psi + \frac{k_{\psi H}^2 - v^2}{k_{\psi H}^2}\left(l_{\psi_d}\dot{\psi}_d - l_{\partial k\psi}\dot{k}_{\psi H}\right)\right)/\cos\phi, \tag{40}$$

where k_ψ is a positive constant and $l_{\partial k\psi} = l_{\partial k\psi 1} - l_{\partial k\psi 2} - l_{\partial k\psi 3}$.

Remark 6: Because of the effects of the roll restoring moment, ϕ can not reach $\pm 90^\circ$. Therefore, the virtual control law (40) is well defined.

By invoking the virtual control law r_d into (32), we have

$$\dot{V}_\psi(\cdot) = -k_\psi \frac{k_{\psi H}^2 e_\psi^2}{k_{\psi H}^2 - \psi^2} + \frac{e_r k_{\psi H}^2 e_\psi}{k_{\psi H}^2 - \psi^2}\cos\phi, \tag{41}$$

where $e_r = r - r_d$ is the yaw angular velocity tracking error and $k_{\psi H}^2 e_\psi r_e \cos\phi / \left(k_{\psi H}^2 - \psi^2\right)$ will be stabilized in the next subsection.

The result in (41) will be used to complete stability analysis of the motion system in Subsection 3.4.

3.3. Yaw angular velocity control

The yaw angular velocity of the hovercraft is an important indicator of safe navigation. If yaw angular velocity exceeds the corresponding safety boundary, the motion control system will become unstable, even it may lead to a capsizing accident. Therefore, we design a time-varying iBLF with considering model uncertainty such that the yaw angular velocity r converges to the desired target r_d while ensuring that the yaw angular velocity remains within safety boundary [33] relating the surge speed.

Considering dynamic model (1), the time derivative of e_r is

$$\dot{e}_r = \frac{M_{zD0}}{J_{z0}} + \Theta_r^T f_r + \frac{\tau_r}{J_{z0}} - \dot{r}_d. \tag{42}$$

The time-varying iBLF with considering model uncertainty is constructed as

$$V_r(e_r, k_{rH}, r_d) = \int_0^{e_r} \frac{\sigma k_{rH}^2}{k_{rH}^2 - (\sigma + r_d)^2} d\sigma + \frac{1}{2}\tilde{\Theta}_r^T \Gamma_r^{-1} \tilde{\Theta}_r, \tag{43}$$

where $\tilde{\Theta}_r = \Theta_r - \hat{\Theta}_r$ is estimation error with $\hat{\Theta}_r$ signifying the estimated value of Θ_r. We define $V_r(\cdot) \overset{def}{=} V_r(e_r, k_{rH}, r_d)$ for convenience's sake in writing.

The derivative of (43) with respect to time, is given by

$$\begin{aligned}\dot{V}_r(\cdot) &= \frac{\partial V_r}{\partial e_r}\dot{e}_r + \frac{\partial V_r}{\partial r_d}\dot{r}_d + \frac{\partial V_r}{\partial k_{rH}}\dot{k}_{rH} - \tilde{\Theta}_r^T \Gamma_r^{-1}\dot{\hat{\Theta}}_r \\ &= \frac{k_{rH}^2 e_r}{k_{rH}^2 - r^2}\left(\frac{M_{zD0}}{J_{z0}} + \Theta_r^T f_r + \frac{\tau_r}{J_{z0}} - \dot{r}_d\right) \\ &\quad + e_r\left(\frac{k_{rH}^2}{k_{rH}^2 - r^2} - l_{r_d}\right)\dot{r}_d - \tilde{\Theta}_r^T \Gamma_r^{-1}\dot{\hat{\Theta}}_r \\ &\quad + e_r\left(l_{\partial kr1} - l_{\partial kr2} - l_{\partial kr3}\right)\dot{k}_{rH},\end{aligned} \tag{44}$$

where

$$l_{r_d} = \frac{k_{rH}}{2e_r}\ln\frac{(k_{rH} + r)(k_{rH} - r_d)}{(k_{rH} - r)(k_{rH} + r_d)}, \tag{45}$$

$$l_{\partial kr1} = \frac{k_{rH}}{e_r}\ln\left(\frac{k_{rH}^2 - r_d^2}{k_{rH}^2 - r^2}\right), \tag{46}$$

$$l_{\partial kr2} = \frac{1}{2}\frac{r_d}{e_r}\ln\frac{(k_{rH} + r)(k_{rH} - r_d)}{(k_{rH} - r)(k_{rH} + r_d)}, \tag{47}$$

$$l_{\partial kr3} = \frac{k_{rH} r}{k_{rH}^2 - r^2}. \tag{48}$$

Remark 7: According to L'Hopital's rule, $|r_d| < k_{rH}$ in Assumption 1, and considering (45), (46) and (47), l_{r_d}, $l_{\partial kr1}$ and $l_{\partial kr2}$ are well defined when $e_r \neq 0$. When $e_r = 0$, we have

$$\lim_{e_r \to 0} l_{r_d} = \frac{k_{rH}^2}{k_{rH}^2 - r_d^2}, \tag{49}$$

$$\lim_{e_r \to 0} l_{\partial kr1} = \frac{2k_{rH} r_d}{k_{rH}^2 - r_d^2}, \tag{50}$$

$$\lim_{e_r \to 0} l_{\partial kr2} = \frac{k_{rH} r_d}{k_{rH}^2 - r_d^2}, \tag{51}$$

therefore, l_{r_d}, $l_{\partial kr1}$ and $l_{\partial kr2}$ are well defined as well.

Then we design the yaw control law and the adaptive updating law of uncertainty parameter as

$$\begin{aligned}\tau_r = J_{z0}\Bigg(&-k_r e_r - \frac{M_{zD0}}{J_{z0}} - \hat{\Theta}_r^T f_r + \frac{k_{rH}^2 - r^2}{k_{rH}^2} l_{r_d}\dot{r}_d \\ &- \frac{k_{rH}^2 - r^2}{k_{rH}^2} l_{\partial kr}\dot{k}_{rH} - \frac{k_{rH}^2 - r^2}{k_{rH}^2}\frac{k_{\psi H}^2 e_\psi}{k_{\psi H}^2 - \psi^2}\cos\phi\Bigg),\end{aligned} \tag{52}$$

$$\dot{\hat{\Theta}}_r = \Gamma_r\left(\frac{k_{rH}^2 e_r}{k_{rH}^2 - r^2} f_r - \sigma_r \hat{\Theta}_r\right), \tag{53}$$

where $l_{\partial kr} = l_{\partial kr1} - l_{\partial kr2} - l_{\partial kr3}$, $\Gamma_r \in R^{n_r \times n_r}$ is a positive definite diagonal matrix and σ_r is a positive constant.

Substituting (52) and (53) into (44) yields

$$\dot{V}_r(\cdot) = -k_r\frac{k_{rH}^2 e_r^2}{k_{rH}^2 - r^2} - \frac{k_{\psi H}^2 e_\psi e_r}{k_{\psi H}^2 - \psi^2}\cos\phi + \sigma_r \tilde{\Theta}_r^T \hat{\Theta}_r$$

$$\leq -k_r\frac{k_{rH}^2e_r^2}{k_{rH}^2-r^2}-\frac{k_{\psi H}^2e_\psi e_r}{k_{\psi H}^2-\psi^2}\cos\phi - \frac{\sigma_r}{2}\tilde{\Theta}_r^T\tilde{\Theta}_r+\frac{\sigma_r}{2}\Theta_r^T\Theta_r. \tag{54}$$

The result in (54) will be utilized for the stability analysis of motion controllers in the next subsection.

3.4. Stability analysis

Next, we summarize the major results of this paper.

Theorem 4: Consider the hovercraft model (1) with safety constraints and system uncertainties, and suppose that Assumption 1-3 are satisfied. If the surge control law is calculated by (23), the virtual heading control law is designed as (40), the yaw control law is expressed by (52) and uncertain parameters are estimated by (24) and (53), then the motion control system is developed in this paper such that: the surge speed is greater than the resistance hump speed, the hovercraft sails in the pre-specified safety heading angles and the yaw angular velocity remains within the safety boundaries relating to the surge speed, as well as all the tracking errors converge to a small region around zero.

Proof: Assign the complete Lyapunov function of the motion control system as

$$V=V_u+V_\psi+V_r. \tag{55}$$

In virtue of (29), (41) and (54), we can obtain the derivative of V as

$$\dot{V}\leq -k_u\frac{u^2e_u^2}{u^2-k_{uL}^2}-k_\psi\frac{k_{\psi H}^2e_\psi^2}{k_{\psi H}^2-\psi^2}-k_r\frac{k_{rH}^2e_r^2}{k_{rH}^2-r^2} -\frac{\sigma_u}{2}\tilde{\Theta}_u^T\tilde{\Theta}_u-\frac{\sigma_r}{2}\tilde{\Theta}_r^T\tilde{\Theta}_r +\frac{\sigma_u}{2}\Theta_u^T\Theta_u+\frac{\sigma_r}{2}\Theta_r^T\Theta_r. \tag{56}$$

According to Theorem 1-2, we further have

$$\dot{V}\leq -\rho V+\varepsilon, \tag{57}$$

where

$$\rho=\min\left\{k_u,k_\psi,k_r,\sigma_u\lambda_{\min}(\Gamma_u),\sigma_r\lambda_{\min}(\Gamma_r)\right\}, \quad \varepsilon=\frac{\sigma_u}{2}\Theta_u^T\Theta_u+\frac{\sigma_r}{2}\Theta_r^T\Theta_r, \tag{58}$$

with $\lambda_{\min}(\cdot)$ denoting the minimum eigenvalue of the matrix $\cdot$.

Solving the inequality (57) yields

$$0\leq V\leq\left(V(0)-\frac{\varepsilon}{\rho}\right)e^{-\rho t}+\frac{\varepsilon}{\rho}. \tag{59}$$

It is obvious that V is uniformly ultimately bounded from (59). Then, according to Theorem 1-2 we have

$$\frac{e_u^2}{2}\leq\int_0^{e_u}\frac{\sigma(\sigma+u_d)^2}{(\sigma+u_d)^2-k_{uL}^2}d\sigma \leq\left(V(0)-\frac{\varepsilon}{\rho}\right)e^{-\rho t}+\frac{\varepsilon}{\rho}, \tag{60}$$

$$\frac{e_i^2}{2}\leq\int_0^{e_i}\frac{\sigma k_{iH}^2}{k_{iH}^2-(\sigma+i_d)^2}d\sigma \leq\left(V(0)-\frac{\varepsilon}{\rho}\right)e^{-\rho t}+\frac{\varepsilon}{\rho}, \tag{61}$$

where $i=\psi,r$. Further, there are $|e_j|\leq\sqrt{2\Xi}, j=u,\psi,r$ and $\left\|\tilde{\Theta}_k\right\|\leq\sqrt{2\Xi/\lambda_{\min}\left(\Gamma_k^{-1}\right)}$, $k=u,r$ with $\Xi:=\left(V(0)-\frac{\varepsilon}{\rho}\right)e^{-\rho t}+\frac{\varepsilon}{\rho}$.

According to the boundedness of V, we infer that there is a positive constant k_V such that $V\leq k_V$. From the definition of iBLF, we know that as $V(t)\to\infty$ only if $|\psi|\to k_{\psi H}$ or $|r|\to k_{rH}$ or $u\to k_{uL}$. Accordingly, we know that $|\psi|\neq k_{\psi H}$, $|r|\neq k_{rH}$ and $u\neq k_{uL}$. In light of Assumption 3, Theorem 3 proposed in this paper, and Lemma 3 in [28], we can conclude that $u>k_{uL}$, $|\psi|<k_{\psi H}$ and $|r|<k_{rH}$ for $\forall t\geq 0$. The proof of Theorem 3 is completed. □

Remark 8: Compared with previous works in [17–25], the yaw control law τ_r and virtual heading control law r_d designed in this paper handle directly time-varying constraints on system states r and ψ in order to satisfy the requirement of safe navigation. Furthermore, the surge control scheme proposed in this paper can ensure that the surge speed is always beyond the resistance hump speed, this scheme is different from all the existing iBLF control schemes [26–31], as far as authors know.

Remark 9: Compared with previous work in [34], the log-type BLF cannot constrain directly the system state, accordingly, an additional mapping to state space is needed. However, in this paper, the proposed iBLF allowing the system state constraints to be mixed with error terms to directly constrain the state signals. In addition, the constraint boundary k_e is time-invariant in [34]. The time-varying BLF technique is more general and complicated than the time-invariant BLF technique. The time-varying iBLF-based control approach has a wider application range in this paper.

Remark 10: Compared with previous works in [35–37], we discovered that the time delays on the inputs generally exist in the control of nonlinear systems. It can lead to the consequence of overshoot increasing, stability time increasing, and even oscillation, divergence and instability of the systems. By presenting a discrete variable transformation, the discrete-time system with time delays on the inputs is transformed into an equivalent non-delay system. Then, the tracking control problem for a class of discrete-time systems with input delays is transformed into the optimal tracking problem for a non-delay system [36,37]. For the hovercraft control, it takes some time for the actuators: air rudders and air propellers to respond to the control signal. However, the simulation results show that

the proposed approach is robust to time delays on the inputs. Some methods to deal with the time delays on inputs will be applied to the hovercraft motion control in future works.

4. SIMULATION RESULTS

In this section, the performance of the proposed motion control system is demonstrated on an underactuated hovercraft. In this case, the surge speed, heading angle and yaw angular velocity are constrained. In simulations, the reader can refer to [2,32] for obtaining details of the main parameters of the hovercraft. The initial values of the hovercraft model are chosen in the pre-specified constrained state space as: $u(0)=30$, $\psi(0)=30$, $r(0)=0$ and the control parameters are set as: $k_u=4$, $k_\psi=1.099$, $k_r=80$. The units of the speed, attitude angle, and angular velocity are kn, deg, and deg/s in this paper, respectively. The initial values of unknown vectors are selected as $\hat{\theta}_u(0)=[0.2,0.1]^T$ and $\hat{\theta}_r(0)=[0.1,0.3]^T$. The parameters of the adaptive updating are selected as $\sigma_u=0.9$, $\sigma_r=0.1$, $\Gamma_u=diag\{2,2\}$ and $\Gamma_r=diag\{6,6\}$. In order to show the feasibility and universality of the proposed scheme, we divide the simulation study into three cases:

Case 1: In the first case, the desired values of the surge speed, heading angle are $u_d=30$ and $\psi_d=40$, respectively. The boundaries of the state constraint are $k_{uL}=sin(0.02t)+26$, $k_{\psi H}=43+cos(0.03t)$, $k_{rH}=15/8-u^2/800$. The time-varying yaw angular velocity constraint adopted in this paper is similar to those in [33] to ensure safety turning motion under high speed. Accordingly, the control laws and the desired yaw angular velocity become the following form:

$$\tau_u = m_0\left(-k_u e_u - vr - \frac{F_{xD0}}{m_0} - \hat{\Theta}_u^T f_u - \frac{u^2-k_{uL}^2}{u^2}\left(l_{\partial ku1}+l_{\partial ku2}-l_{\partial ku3}\right)\dot{k}_{uL}\right), \tag{62}$$

$$\tau_r = J_{z0}\left(-k_r e_r - \frac{M_{zD0}}{J_{z0}} - \hat{\Theta}_r^T f_r + \frac{k_{rH}^2-r^2}{k_{rH}^2}l_{r_d}\dot{r}_d - \frac{k_{rH}^2-r^2}{k_{rH}^2}l_{\partial kr}\dot{k}_{rH} - \frac{k_{rH}^2-r^2}{k_{rH}^2}\frac{k_{\psi H}^2 e_\psi}{k_{\psi H}^2-\psi^2}\cos\phi\right), \tag{63}$$

$$r_d = \left(-k_\psi e_\psi - \frac{k_{\psi H}^2-\psi^2}{k_{\psi H}^2}l_{\partial k\psi}\dot{k}_{\psi H}\right)\Big/\cos\phi. \tag{64}$$

We know that the above control scheme is similar to those in [23], which deal with a time-varying constraint on state variables. However, the desired targets u_d and ψ_d are time-invariant, in addition, the constraint on state u is $u>k_{uL}$ in this paper.

The simulation results of Case 1 are shown in Figs. 3-7. It is obvious from Figs. 3-5 that the desired time-invariant

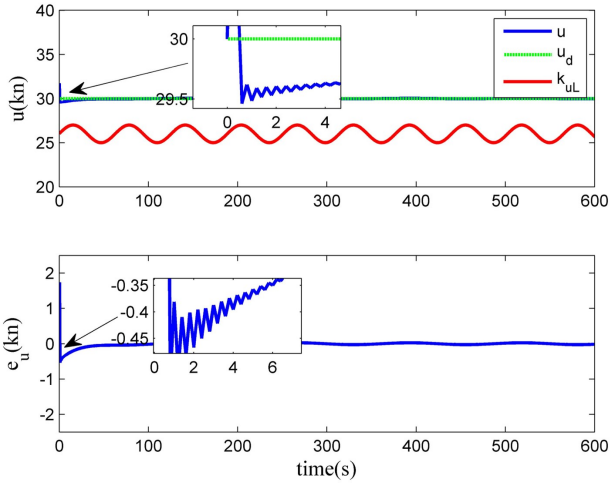

Fig. 3. Tracking performance and tracking error of the surge speed under Case 1.

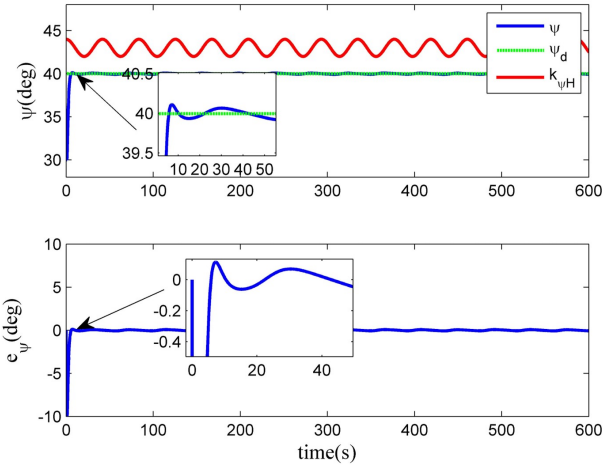

Fig. 4. Tracking performance and tracking error of the heading angle under Case 1.

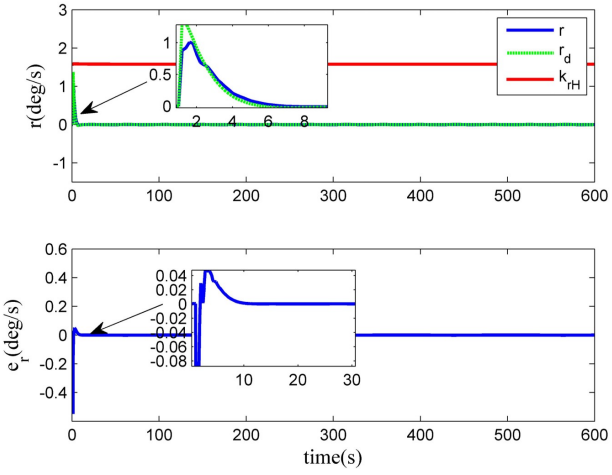

Fig. 5. Tracking performance and tracking error of the yaw angular velocity under Case 1.

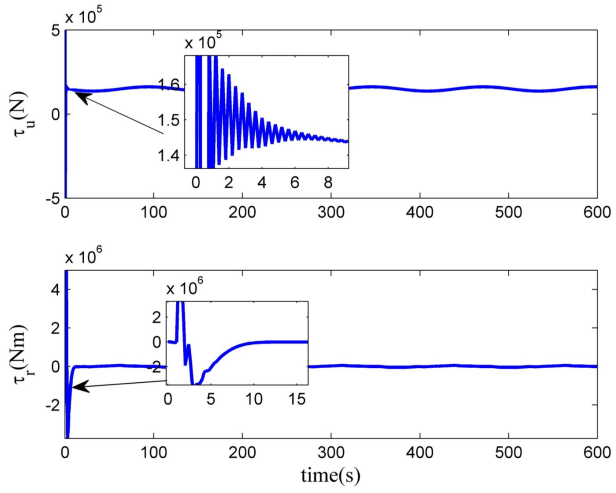

Fig. 6. Control input under Case 1.

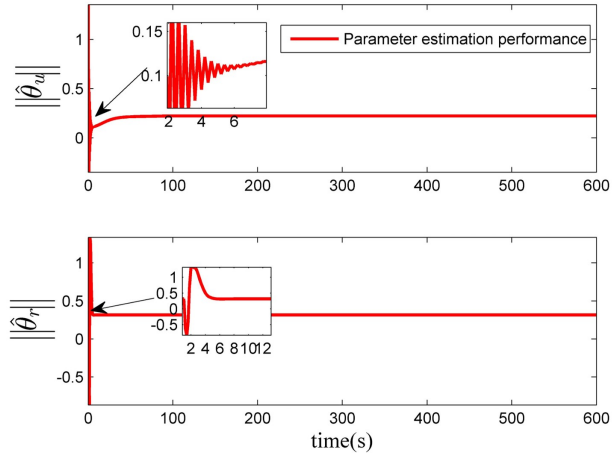

Fig. 7. Parameter estimation performance under Case 1.

targets u_d, ψ_d can be tracked in ideal accuracy and the time-varying virtual control law r_d can be tracked as well. And for the purpose of safety navigation, the surge speed can be limited above the lowest safe boundary k_{uL}, the heading angle can be constrained within prescribed safety heading angles $k_{\psi H}$ and the time-varying constraint k_{rH} on the yaw angular velocity is never violated. The tracking errors can converge to a small region containing zero from further observation. The curves of the control input vary with time are shown in Fig. 6. From the adaptive updating laws (24), (53) and Fig. 7, we know that the adaptive parameter estimation performance has a large deviation due to the large state tracking errors e_u and e_r in the initial tracking stage. After 10 seconds, the adaptive parameters basically achieved tracking the desired setting values, namely, we have that $\hat{\theta}_u = \theta_u$ and $\hat{\theta}_r = \theta_r$. Therefore, by analyzing simulation results, we know that the proposed motion control scheme can complete that the states converge to the desired time-invariant targets while ensuring that the corresponding states remain within the predefined time-varying safety constraint boundaries.

Case 2: In the second case, the desired values of the surge speed, heading angle are $u_d = 30 + 2cos(0.02t)$ and $\psi_d = 39 + cos(0.01t)$, respectively. The boundaries of the state constraint are $k_{uL} = 26$, $k_{\psi H} = 43$, and $k_{rH} = 1.5$. Then the control laws and the desired yaw angular velocity become the following form:

$$\tau_u = m_0 \left(-k_u e_u - vr - \frac{F_{xD0}}{m_0} - \hat{\Theta}_u^T f_u - \frac{u^2 - k_{uL}^2}{u^2} l_{u_d} \dot{u}_d \right), \tag{65}$$

$$\tau_r = J_{z0} \left(-k_r e_r - \frac{M_{zD0}}{J_{z0}} - \hat{\Theta}_r^T f_r + \frac{k_{rH}^2 - r^2}{k_{rH}^2} l_{r_d} \dot{r}_d - \frac{k_{rH}^2 - r^2}{k_{rH}^2} \frac{k_{\psi H}^2 e_\psi \cos\phi}{k_{\psi H}^2 - \psi^2} \right), \tag{66}$$

$$r_d = \left(-k_\psi e_\psi + \frac{k_{\psi H}^2 - v^2}{k_{\psi H}^2} l_{\psi_d} \dot{\psi}_d \right) \Big/ \cos\phi. \tag{67}$$

The above control scheme is analogous to those in [24], which only completes time-invariant constraints on system states. However, the proposed scheme can ensure the time-varying constraint on states in this paper.

The simulation results of Case 2 are presented in Figs. 8-12. In Figs. 8-10, the desired time-varying targets u_d, ψ_d, and time-varying virtual control law r_d can be tracked by the corresponding states in ideal accuracy. Considering safety navigation, the surge speed can be constrained above the resistance hump speed k_{uL}, the heading and the yaw angular velocity never surpass the corresponding time-invariant safety boundaries $k_{\psi H}$ and k_{rH}, respectively. In Fig. 11, the control inputs are given. From the adaptive updating laws (24), (53) and Fig. 12, we know

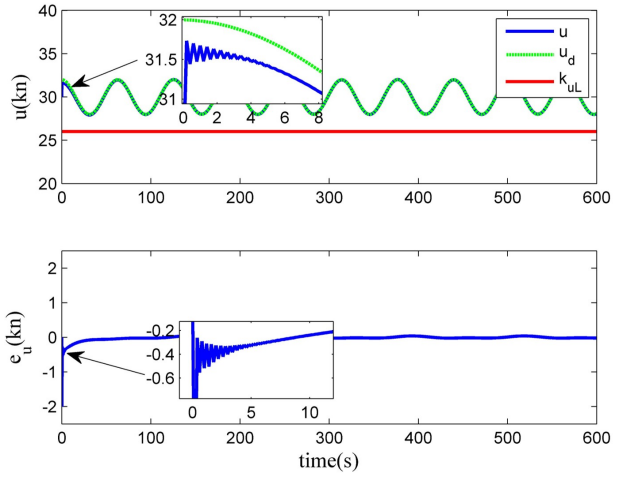

Fig. 8. Tracking performance and tracking error of the surge speed under Case 2.

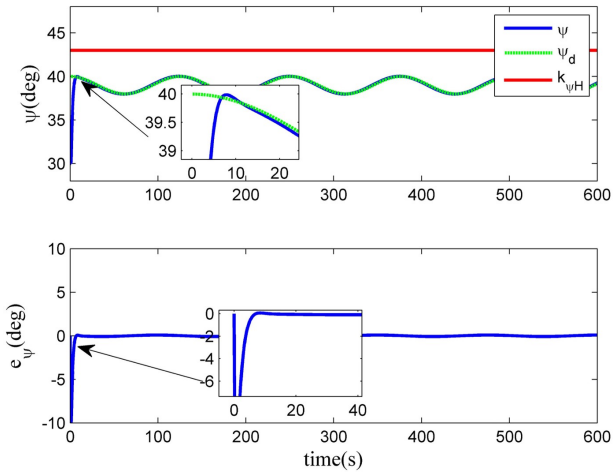

Fig. 9. Tracking performance and tracking error of the heading angle under Case 2.

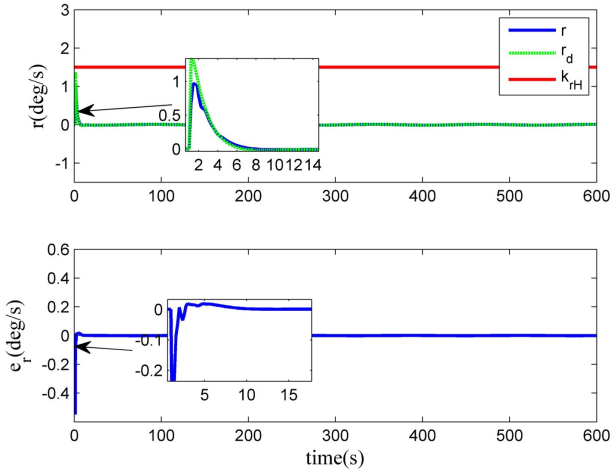

Fig. 10. Tracking performance and tracking error of the yaw angular velocity under Case 2.

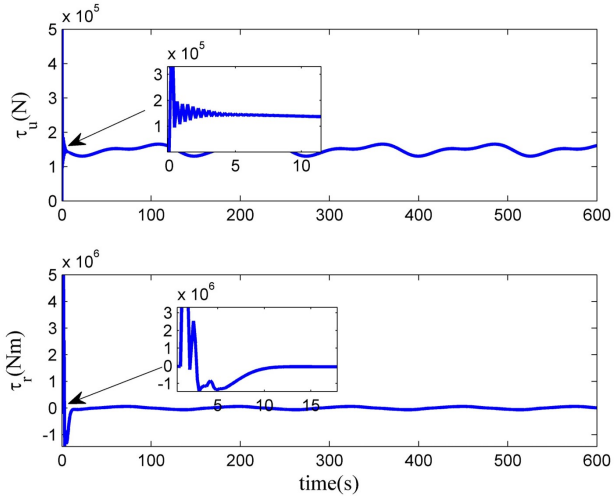

Fig. 11. Control input under Case 2.

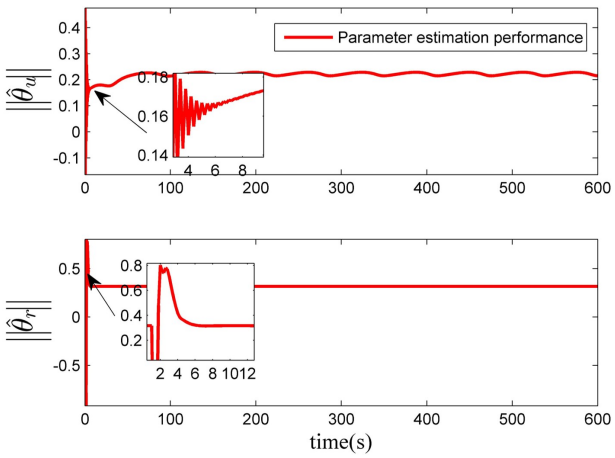

Fig. 12. Parameter estimation performance under Case 2.

that the adaptive parameter estimation performance has a large deviation due to the large state tracking errors e_u and e_r in the initial tracking stage. After 10 seconds, the adaptive parameters basically achieved tracking the desired setting values, namely, we have that $\hat{\theta}_u = \theta_u$ and $\hat{\theta}_r = \theta_r$. According to the above analysis, we can summarize that the motion control system designed in this paper can realize the system states move along the desired time-varying targets while making the corresponding states stay always within the considered time-invariant safety limits.

Case 3: In the third case, the desired values of the surge speed and heading angle are $u_d = 30 + 2cos(0.02t)$ and $\psi_d = 39 + cos(0.01t)$, respectively. The boundaries of the state constraint are $k_{uL} = sin(0.02t) + 26$, $k_{\psi H} = 43 + cos(0.03t)$, and $k_{rH} = 15/8 - u^2/800$. The control laws and the desired yaw angular velocity are expressed by (26), (52) and (40), respectively. The simulation results of Case 4 are presented in Figs. 13-17. In Figs. 13-15, the system states of the hovercraft have been able to move accurately along desired time-varying target trajectories u_d, ψ_d and the virtual time-varying stability function r_d. At the same time, the time-varying constraints on the surge speed guaranteeing the lowest safety boundary never be violated, the heading of the hovercraft is always kept in the pre-specified time-varying safety range and the yaw angular velocity remains within the time-varying safety boundary as well. The control inputs are shown in Fig. 16. From the adaptive updating laws (24), (53) and Fig. 17, we know that the adaptive parameter estimation performance has a large deviation due to the large state tracking errors e_u and e_r in the initial tracking stage. After 10 seconds, the adaptive parameters basically achieved tracking the desired setting values, namely, we have that $\hat{\theta}_u = \theta_u$ and $\hat{\theta}_r = \theta_r$. Accordingly, the simulation results can be summarized as the control laws (23), (52) and (40) designed in this paper can realize that the system states track accurately the desired time-varying targets while ensuring that

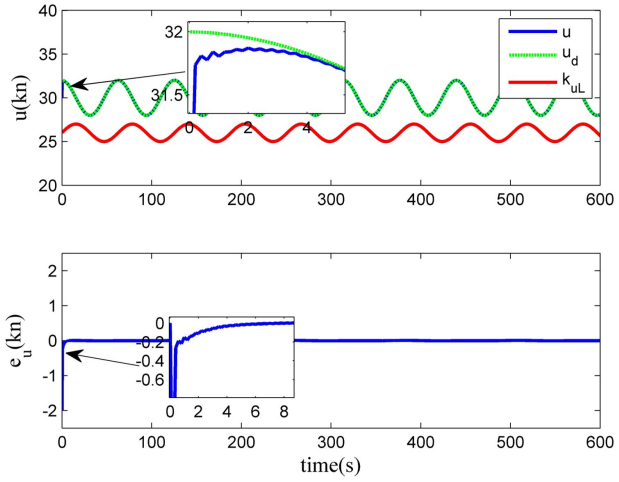

Fig. 13. Tracking performance and tracking error of the surge speed under Case 3.

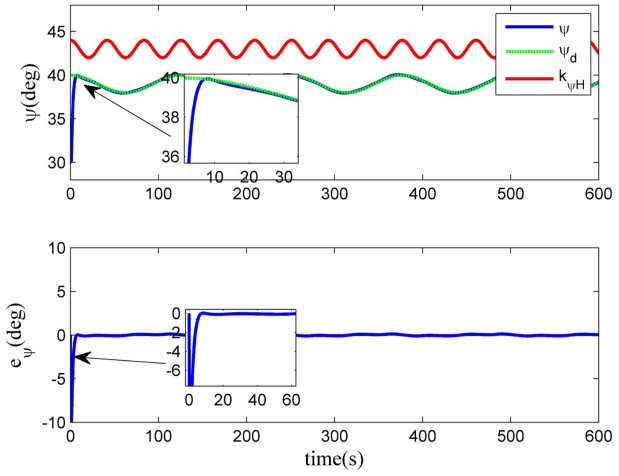

Fig. 14. Tracking performance and tracking error of the heading angle under Case 3.

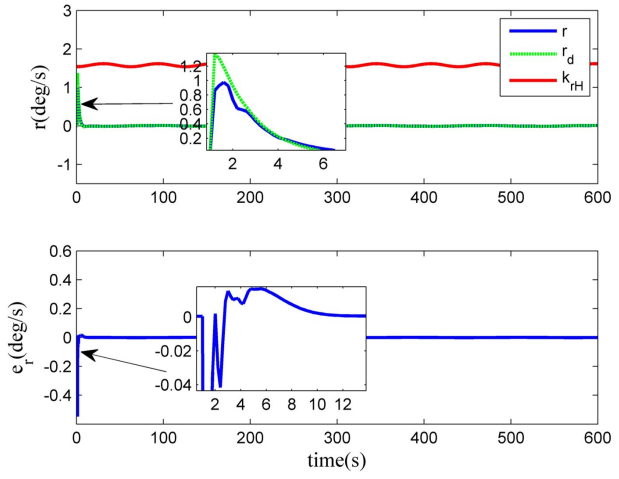

Fig. 15. Tracking performance and tracking error of the yaw angular velocity under Case 3.

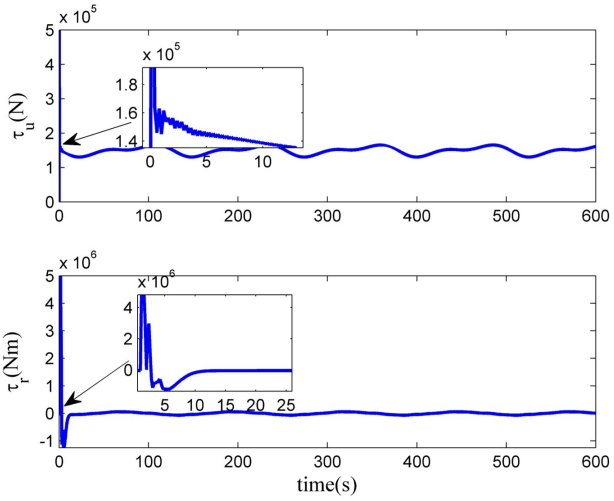

Fig. 16. Control input under Case 3.

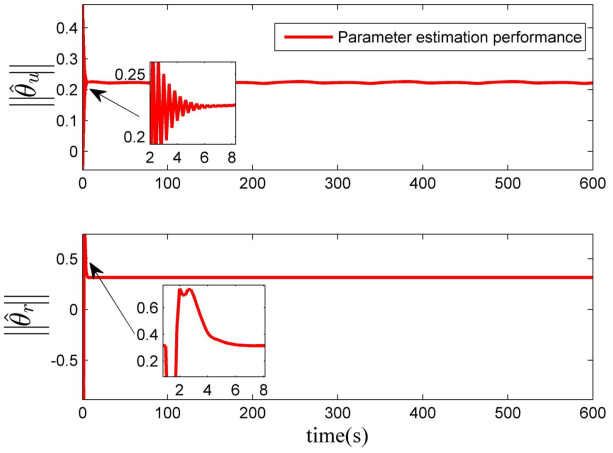

Fig. 17. Parameter estimation performance under Case 3.

the corresponding states are constrained always within the considered time-varying safety boundaries.

5. CONCLUSION

This study aims at developing an adaptive safety motion control schemes for a hovercraft with multiple safety constraints and model uncertainties. The surge speed has been constrained effectively to exceed always the resistance hump speed by virtue of the improved iBLF-based control method. By introducing the time-varying iBLF, the yaw angular velocity is successfully constrained to the interior of a time-varying safety boundary relating the surge speed to perform the safety turning under the high surge speed, as well as the heading is limited within the pre-specified safety region. And the model uncertainties are handled very well by designing an adaptive parameter approximation algorithm. Three different simulations are completed to verify the effectiveness and universality of

the proposed control schemes.

REFERENCES

[1] M. Cohen, T. Miloh, and G. Zilman, "Wave resistance of a hovercraft moving in water with nonrigid bottom," *Ocean Engineering*, vol. 128, no. 11, pp. 1461-1478, Nov. 2001.

[2] M. Fu, S. Gao, C. Wang, and M. Li, "Design of driver assistance system for air cushion vehicle with uncertainty based on model knowledge neural network," *Ocean Engineering*, vol. 172, no. 11, pp. 296-307, Jan. 2019.

[3] H. Sira-Ramirez, "Dynamic second-order sliding mode control of the hovercraft vessel," *IEEE Trans. on Control Systems Technology*, vol. 10, no. 6, pp. 860-865, Nov. 2002.

[4] J. Zhao and J. Pang, "Trajectory control of underactuated hovercraft," *Proc. of 8th World Congress on Intelligent Control and Automation*, no. 6, pp. 3904-3907, Jul. 2010.

[5] R. Morales, H. Sira-Ramirez, and J. A. Somolinos, "Linear active disturbance rejection control of the hovercraft vessel model," *Ocean Engineering*, vol. 96, no. 6, pp. 100-108, Mar. 2015.

[6] G. G. Rigatos and G. V. Raffo, "Input-output linearizing control of the underactuated hovercraft using the derivative-free nonlinear Kalman filter," *Unmanned Systems*, vol. 03, no. 02, pp. 127-142, Mar. 2015.

[7] D. Q. Mayne and H. Michialska, "Receding horizon control of nonlinear systems," *IEEE Trans. on Automatic Control*, vol. 35, no. 7, pp. 814-824, Jul. 1990.

[8] W. B. Dunbary and R. M. Murray, "Distributed receding horizon control with application to multi-vehicle formation stabilization," *Automatica*, vol. 42, no. 4, pp. 549-558, Dec. 2006.

[9] E. Rimon and D. E. Koditschek, "Exact robot navigation using artificial potential functions," *IEEE Trans. on Robotics and Automation*, vol. 8, no. 5, pp. 501-518, Oct. 1992.

[10] J. Guldner and V. I. Utkin, "Sliding mode control for gradient tracking and robot navigation using artificial potential fields," *IEEE Trans. on Robotics and Automation* , vol. 11, no. 2, pp. 247-254, Apr. 1995.

[11] Z. Li, J. Sun, and S. Oh, "Path following for marine surface vessels with rudder and roll constraints: An MPC approach," *Proc. Amer. Control Conf.*, pp. 3611-3613, Jun. 2009.

[12] D. Q. Mayne, J. B. Rawlings, C. V. Rao, and P. O. M. Scokaert, "Constrained model predictive control: Stability and optimality," *Automatica*, vol. 36, no. 6, pp. 789-814, 2000.

[13] A. Caliciotti and L. R. Celsi, "On optimal buffer allocation for guaranteeing quality of service in multimedia internet broadcasting for mobile networks," *International Journal of Control, Automation and Systems*, vol. 17, no. 11, pp. 2819-2832, May 2020.

[14] M. Islam, M. Okasha, and E. Sulaeman, "A model predictive control (MPC) approach on unit quaternion orientation based quadrotor for trajectory tracking," *International Journal of Control, Automation and Systems*, vol. 17, no. 11, pp. 2819-2832, Nov. 2019.

[15] M. Yue, C. An, and J.-Z. Sun, "An efficient model predictive control for trajectory tracking of wheeled inverted pendulum vehicles with various physical constraints," *International Journal of Control, Automation and Systems*, vol. 16, no. 1, pp. 265-274, Feb. 2018.

[16] C. Liu, J. Gao, and D. Xu, "Lyapunov-based model predictive control for tracking of nonholonomic mobile robots under input constraints," *International Journal of Control, Automation and Systems*, vol. 15, no. 5, pp. 2313-2319, Oct. 2017.

[17] S. Zhang, Y. Dong, Y. Ouyang, Z. Yin, and K. Peng, "Adaptive neural control for robotic manipulators with output constraints and uncertainties," *IEEE Trans. on Neural Networks and Learning Systems*, vol. 29, no. 11, pp. 5554-5564, Nov 2018.

[18] H. Li, L. Bai, L. Wang, Q. Zhou, and H. Wang, "Adaptive neural control of uncertain nonstrict-feedback stochastic nonlinear systems with output constraint and unknown dead zone," *IEEE Trans. on Systems, Man, and Cybernetics: Systems*, vol. 47, no. 8, pp. 2048-2059, Aug. 2017.

[19] X. He, W. He, J. Shi, and C. Sun, "Boundary vibration control of variable length crane systems in two-dimensional space with output constraints," *IEEE/ASME Trans. on Mechatronics*, vol. 22, no. 5, pp. 1952-1962, Oct. 2017.

[20] Y. J. Liu, S. Lu, D. Li, and S. Tong, "Adaptive controller design-based ABLF for a class of nonlinear time-varying state constraint systems," *IEEE Trans. on Systems, Man, and Cybernetics: Systems*, vol. 47, no. 7, pp. 1546-1553, Jul. 2017.

[21] M. A. Rami and D. Napp, "Discrete-time positive periodic systems with state and control constraints," *IEEE Trans. on Automatic Control* , vol. 61, no. 1, pp. 234-239, Jan. 2016.

[22] J. Yu, L. Zhao, H. Yu, and C. Lin, "Barrier Lyapunov functions-based command filtered output feedback control for full-state constrained nonlinear systems," *Automatica*, vol. 105, no. 1, pp. 71-79, Jul. 2019.

[23] Z. Zheng, L. Ruan, and M. Zhu, "Output-constrained tracking control of an underactuated autonomous underwater vehicle with uncertainties," *Ocean Engineering*, vol. 175, no. 1, pp. 241-250, Mar 2019.

[24] Z. Zheng, L. Sun, and L. Xie, "Error-constrained LOS path following of a surface vessel with actuator saturation and faults, " *IEEE Trans. on Systems, Man, and Cybernetics: Systems*, vol. 48, no. 10, pp. 1794-1805, Oct. 2018.

[25] X. Jin, "Adaptive fault tolerant control for a class of input and state constrained MIMO nonlinear systems," *International Journal of Robust and Nonlinear Control*, vol. 26, no. 2, pp. 286-302, Jan. 2016.

[26] J. Zhang, "Integral barrier Lyapunov functions-based neural control for strict-feedback nonlinear systems with multi-constraint," *International Journal of Control, Automation and Systems*, vol. 16, no. 4, pp. 2002-2010, Aug. 2018.

[27] L. Kong, W. He, C. Yang, Z. Li, and C. Sun, "Adaptive fuzzy control for coordinated multiple robots with constraint using impedance learning," *IEEE Trans. on Cybernetics*, vol. 49, no. 8, pp. 3052-3063, Aug. 2019.

[28] Z. L. Tang, S. S. Ge, K. P. Tee, and W. He, "Robust adaptive neural tracking control for a class of perturbed uncertain nonlinear systems with state constraints," *IEEE Trans. on Systems, Man, and Cybernetics: Systems*, vol. 46, no. 12, pp. 1618-1629, Dec 2016.

[29] W. He, S. Zhang, and S. S. Ge, "Adaptive control of a flexible crane system with the boundary output constraint," *IEEE Trans. on Industrial Electronics*, vol. 61, no. 8, pp. 4126-4133, Aug. 2014.

[30] W. He and S. S. Ge, "Vibration control of a flexible string with both boundary input and output constraints," *IEEE Trans. on Control Systems Technology*, vol. 23, no. 4, pp. 1245-1254, Jul. 2015.

[31] Y. Liu, S. Tong, C. L. P. Chen, and D. Li, "Adaptive NN control using integral barrier Lyapunov functionals for uncertain nonlinear block-triangular constraint systems," *IEEE Trans. on Cybernetics*, vol. 47, no. 11, pp. 3747-3757, Nov. 2017.

[32] M. Fu, S. Gao, C. Wang, and M. Li, "Human-centered automatic tracking system for underactuated hovercraft based on adaptive chattering-free full-order terminal sliding mode control," *IEEE Access*, vol. 6, no. 4, pp. 37883-37892, Jul. 2018.

[33] R. Gran, G. Carpenter, and R. Klein, "Computer aided design of a control system for a hovercraft," *in 1982 21st IEEE Conference on Decision and control*, no. 6, pp. 1347-1353, Dec. 1982.

[34] M. Fu, T. Wang, and C. Wang, "Adaptive neural-based finite-time trajectory tracking control for underactuated marine surface vessels with position error constraint," *IEEE Access,* vol. 7, no. 5, pp. 16309-16322, Oct. 2019.

[35] L. R. Celsi, R. Bonghi, S. Monaco, and D. Normand-Cyrot, "On the exact steering of finite sampled nonlinear dynamics with input delays," *IFAC-PapersOnLine,* vol. 48, no. 11, pp. 674-679, Oct. 2015.

[36] H. Wang and G. Tang, "Observer-based optimal output tracking for discrete-time systems with multiple state and input delays," *International Journal of Control, Automation and Systems,* vol. 7, no. 1, pp. 57-66, Feb. 2009.

[37] S. Han, D. Wang, Y. H. Chen, G. Tang, and X. Yang, "Optimal tracking control for discrete-time systems with multiple input delays under sinusoidal disturbances," *International Journal of Control, Automation and Systems,* vol. 13, no. 2, pp. 292-301, Apr 2015.

Mingyu Fu received her Ph.D. degree from the College of Automation, Harbin Engineering University, Harbin, China, in 2005, where she is currently a Professor and a Ph.D. Supervisor. Her current research interests include vessel dynamic positioning control, automatic control of unmanned surface vehicle, and hovercraft motion control.

Tan Zhang received his M.E. degree from the College of Automation, Harbin Engineering University, Harbin, China, in 2017. He is currently pursuing a Ph.D. degree of control science and engineering in the College of Automation. His current research interests include robust adaptive control and motion control of the hovercraft.

Fuguang Ding received his M.E. degree from the College of Computer Science and Technology, Harbin Engineering University, Harbin, China, in 1996. Currently he is a Professor and an M.E. Supervisor in the College of Automation, Harbin Engineering University. His main research interests include vessel dynamic positioning control, vessel intelligent control, and motion control of high speed vessel.